

## DEVELOPMENT OF A BIODYNAMIC MODEL OF A SEATED HUMAN BODY EXPOSED TO LOW FREQUENCY WHOLE-BODY VIBRATION

Zengkang Gan\*<sup>1</sup>, Andrew J. Hillis<sup>1</sup>, Jocelyn Darling<sup>1</sup>

<sup>1</sup>Centre for Power Transmission and Motion Control, Department of Mechanical Engineering,  
University of Bath, Bath, United Kingdom  
{z.gan, a.j.hillis, j.darling}@bath.ac.uk

**Keywords:** Lumped-parameter models, Seated human body, Biodynamic, Whole-body vibration.

**Abstract.** *In this paper, a lumped-parameter biodynamic model of a seated human body (SHB) exposed to low frequency whole-body vibration in both vertical and fore-and-aft directions is developed. The model is based on all three types of biodynamic functions: seat-to-head transmissibility (STHT), driving-point mechanical impedance (DPMI) and apparent mass (APM). The objective of this work is to match all three functions and to represent the biodynamic behaviour of the SHB in a more comprehensive way. Three sets of synthesized experimental data from published literature are selected as the target values for each of the three biodynamic functions. A curve fitting method is used in the parameter identification process which involves the solution of a multivariable optimization function comprising the root mean square errors between the computed values using the model and those target values. Finally, a numerical simulation of the frequency response of the model in terms of all three biodynamic functions has been carried out. The results show that an improved fit is achieved.*

## 1 INTRODUCTION

The harmful effects on human performance and health caused by low frequency whole-body vibration are of increasing concern. Much evidence has shown that there is a direct relationship between lower back pain and continuous exposure to whole-body vibration [1]. It is also well known that severe vibration may cause neck and spine injuries. In addition, the transmission of unwanted vibration to the human body may lead to fatigue and discomfort.

In order to gain a better understanding of seated human body biodynamic response and adverse effects under low frequency whole-body vibration, a variety of statistical and analytical studies have been carried out by various researchers. Statistical studies usually involve measuring the kinetic and biodynamic responses of human subjects. There are three types of generalized biodynamic response functions - seat-to-head transmissibility (STHT), driving-point mechanical impedance (DPMI) and apparent mass (APM), which are widely used to characterize the biodynamic response of the seated human body under the most commonly encountered vibration environments. The STHT function is defined as the complex ratio of the output vibration level on the head to the input vibration level on the seat in the frequency range of interest [2]. The DPMI function is defined as the complex ratio between the transmitted dynamic force to which the subject is exposed and the input driving-point velocity [3]. The APM function is defined similarly to the DPMI function. It specifies the complex ratio of driving force to the driving-point acceleration. All three functions can be evaluated by calculating the magnitude and phase responses in the frequency range of interest.

The measured biodynamic response data from a statistical study can be used to identify mechanical-equivalent properties of the human body and to help in developing and validating mathematical models for analytical study. In the past few decades, a number of mathematical models have been developed based upon diverse measurements [3, 4]. However, the majority of human body models were derived to satisfy a single biodynamic response function. Such an approach may provide a reasonable fit with the function data being considered, but uncertain matches with the others. Since the biodynamic behaviour of the seated human body is equally characterized by all the three types of functions, it would be more useful for a mathematical model to fit all three biodynamic functions.

In the present paper a synthesis of experimental data for seated human body biodynamic responses in both vertical and fore-and-aft directions in terms of STHT, DPMI and APM is generated. Based on the synthesized data, a lumped-parameter biodynamic model of a seated human body is developed.

## 2 MEASUREMENT DATA OF SEATED HUMAN SUBJECTS

The biodynamic response data of seated human subjects was obtained from a variety of field and experimental measurements which were carried out under widely varying test conditions [2-12]. The variation of test conditions for individual measurements may involve both intrinsic and extrinsic variables, such as subject mass and population, seat posture, feet and hand position, vibration excitation type and level, seat backrest angle and measurement location on the subjects. In order to avoid significant discrepancies among the measurement data associated with the variable conditions, the following requirements were specified for the synthesis of the biodynamic characteristics of seated human subjects [3, 4]: (a) Studies presenting measurements based on at least six subjects; (b) The measured subjects are considered to be sitting in an upright posture, irrespective of the hands' position; (c) Feet are supported and vibrated on the same excitation base; (d) Subject mass is in the range of 45-100 kg; (e) Excitation levels are below  $5 \text{ m/s}^2$  and magnitude and phase data are reported in the 0-20 Hz frequency range; (f) Either sinusoidal or random vibration excitation is used.

Based upon the above requirements, the following published measurement data were selected for the synthesis of seated human body biodynamic properties: [2, 3, 5] for the seat-to-head transmissibility (STHT) data; [3, 6-8] for the driving-point mechanical impedance (DPMI) data; [9-12] for the apparent mass (APM) data. The synthesized data, shown in Table 1 and 2, is derived by averaging the above data sets and applying proper smoothing within the frequency range of interest.

Frequency (Hz)	STHT (abs)		DPMI (N*s/m)		APM (kg)	
	Magnitude	Phase (deg)	Magnitude	Phase (deg)	Magnitude	Phase (deg)
0.5	1.01	-0.2	95	89.5	59	-2.2
0.75	1.00	-0.7	175	89.0	60	-2.3
1.0	1.01	-0.8	310	88.5	60	-3.5
2.0	1.10	-6.0	754	87.5	61	-4.5
3.0	1.16	-10.0	1255	82	71	-10
4.0	1.28	-17.5	2252	66	81	-15
4.5	1.37	-29	2704	45	80	-23
5.0	1.45	-40	2605	31	76	-31
5.5	1.43	-50	2254	23	67	-43
6.0	1.30	-61	2105	23	53	-55
6.5	1.18	-62	1865	20	48	-60
7.0	1.09	-60	1892	22	44	-64
8.0	0.99	-62	1998	21	39	-68
9.0	0.94	-70	2002	20	36	-70
10.0	0.95	-76	2015	16	32	-72
12.0	0.86	-85	1905	17	31	-80
14.0	0.76	-97	1770	18	25	-83
16.0	0.67	-105	1625	19	18	-82
18.0	0.60	-113	1585	20	14	-81
20.0	0.56	-121	1605	20	11	-81

Table 1: Synthesized data of STHT, DPMI and APM mean values in the vertical direction.

Frequency (Hz)	STHT (abs)		DPMI (N*s/m)		APM (kg)	
	Magnitude	Phase (deg)	Magnitude	Phase (deg)	Magnitude	Phase (deg)
0.5	1.26	-1	55	83.0	53.0	-8.0
0.75	1.44	-16	148	80.8	57.0	-10.6
1.0	1.62	-40	257	76.6	59.5	-12.8
1.25	1.59	-64	392	71.6	63.1	-16.0
1.5	1.41	-85	515	65.4	67.2	-20.2
1.75	1.23	-103	655	59.5	69.6	-24.0
2.0	1.10	-119	850	48.4	70.2	-28.5
2.5	0.86	-135	1010	33.6	62.5	-39.4
2.75	0.71	-144	1068	25.0	58.6	-46.0
3.0	0.56	-159	1095	17.1	54.0	-53.5
3.5	0.41	-168	1083	1.8	45.1	-62.5
4.0	0.29	-175	1061	-7.5	37.7	-75.0
4.5	0.26	-189	1028	-15.5	35.3	-80.5
5.0	0.23	-198	974	-21.5	30.6	-81.0
6.0	0.18	-211	912	-25.8	20.5	-86.2
7.0	0.13	-231	853	-29.0	17.4	-91.0

8.0	0.10	-247	746	-29.8	12.9	-90.2
9.0	0.08	-253	647	-29.3	10.3	-87.0
10.0	0.08	-255	555	-28.0	7.8	-85.0
11.0	0.08	-254	521	-27.2	7.2	-84.0
12.0	0.08	-252	487	-25.7	6.0	-84.0

Table 2: Synthesized data of STHT, DPMI and APM mean values in the fore-and-aft direction.

The lower and upper limits of each data are not included in the above tables. However, they will be shown in figures in later sections of the paper. Sufficient measurement data of STHT, DPMI and APM responses in the fore-and-aft direction is only available up to 12 Hz.

### 3 MATHEMATICAL MODEL DEVELOPMENT

#### 3.1 Model description

The proposed model is a lumped-parameter linear spring and damper system. The model includes segments representing appropriate anatomical parts of the body and is capable of accommodating translational and rotational (head and neck joint) movements of these segments, which enable it to represent the measured STHT, DPMI and APM function data under low frequency whole-body vibration.

This model is composed of two sub-models: the vertical model and the fore-and-aft model, as shown in Figure 1. The vertical model consists of five segments: head and neck ( $m_5$ ), upper torso ( $m_4$ ), arms ( $m_3$ ), viscera ( $m_2$ ), and lower torso ( $m_1$ ). The spring ( $k_{41}$ ) and damper ( $c_{41}$ ) connecting the upper and lower torsos represent the body spine. In the fore-and-aft model, the main body mass ( $m_1 + m_2 + m_3 + m_4$ ) is treated as a single lumped mass. The head and neck ( $m_5$ ) and the main body are connected by a rotational degree of freedom. These rigid masses are coupled by linear elastic spring and damping elements. The masses of the lower legs and the feet are not incorporated in the model representation, assuming their negligible contributions to the whole-body biodynamic response.

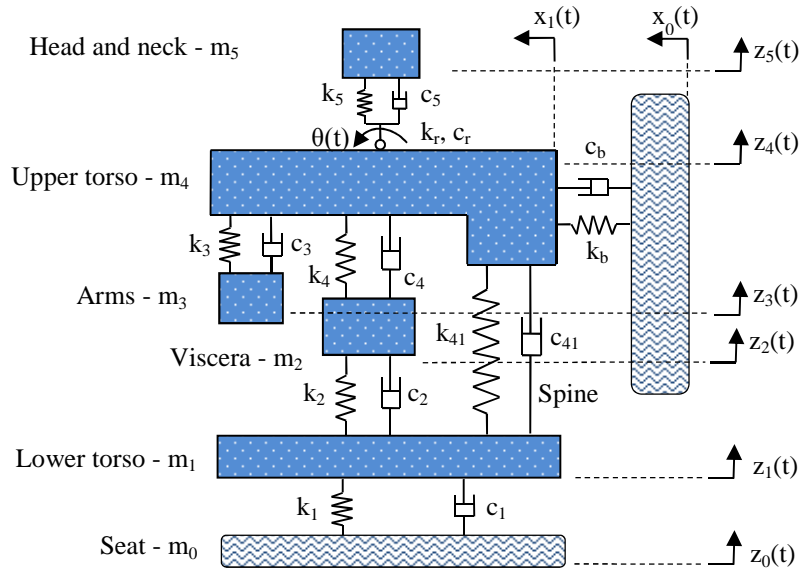


Figure 1: Schematic of model for seated human subjects in both vertical and fore-and-aft directions.

### 3.2 Equations of motion (EOMs)

EOMs of the model are derived from the free-body diagram of each. The vertical model has five degrees of freedom in total: the vertical displacement of each segment  $\{z_1(t), z_2(t), z_3(t), z_4(t), z_5(t)\}$ . The vertical model EOMs can be expressed by the following coupled differential equations in matrix form:

$$[\mathbf{M}]\{\ddot{\mathbf{z}}\} + [\mathbf{C}]\{\dot{\mathbf{z}}\} + [\mathbf{K}]\{\mathbf{z}\} = \{\mathbf{f}_n\} \quad (1)$$

where  $[\mathbf{M}]$ ,  $[\mathbf{C}]$  and  $[\mathbf{K}]$  are mass, damping and stiffness matrices, respectively;  $\{\ddot{\mathbf{z}}\}$ ,  $\{\dot{\mathbf{z}}\}$  and  $\{\mathbf{z}\}$  are acceleration, velocity and displacement vectors, respectively;  $\{\mathbf{f}_n\}$  is the excitation force vector. All the above matrices and vectors can be expressed as follows:

$$[\mathbf{M}] = \begin{bmatrix} m_1 & 0 & 0 & 0 & 0 \\ 0 & m_2 & 0 & 0 & 0 \\ 0 & 0 & m_3 & 0 & 0 \\ 0 & 0 & 0 & m_4 & 0 \\ 0 & 0 & 0 & 0 & m_5 \end{bmatrix};$$

$$[\mathbf{C}] = \begin{bmatrix} c_1 + c_2 + c_{41} & -c_2 & 0 & -c_{41} & 0 \\ -c_2 & c_2 + c_4 & 0 & -c_4 & 0 \\ 0 & 0 & c_3 & -c_3 & 0 \\ -c_{41} & -c_4 & -c_3 & c_3 + c_4 + c_{41} + c_5 & -c_5 \\ 0 & 0 & 0 & -c_5 & c_5 \end{bmatrix};$$

$$[\mathbf{K}] = \begin{bmatrix} k_1 + k_2 + k_{41} & -k_2 & 0 & -k_{41} & 0 \\ -k_2 & k_2 + k_4 & 0 & -k_4 & 0 \\ 0 & 0 & k_3 & -k_3 & 0 \\ -k_{41} & -k_4 & -k_3 & k_3 + k_4 + k_{41} + k_5 & -k_5 \\ 0 & 0 & 0 & -k_5 & k_5 \end{bmatrix};$$

$$\{\ddot{\mathbf{z}}\} = \begin{Bmatrix} \ddot{z}_1 \\ \ddot{z}_2 \\ \ddot{z}_3 \\ \ddot{z}_4 \\ \ddot{z}_5 \end{Bmatrix}; \quad \{\dot{\mathbf{z}}\} = \begin{Bmatrix} \dot{z}_1 \\ \dot{z}_2 \\ \dot{z}_3 \\ \dot{z}_4 \\ \dot{z}_5 \end{Bmatrix}; \quad \{\mathbf{z}\} = \begin{Bmatrix} z_1 \\ z_2 \\ z_3 \\ z_4 \\ z_5 \end{Bmatrix}; \quad \{\mathbf{f}_n\} = \begin{Bmatrix} c_1\dot{z}_0 + k_1z_0 \\ 0 \\ 0 \\ 0 \\ 0 \end{Bmatrix}.$$

The fore-and-aft model has two degrees of freedom in total: the fore-and-aft displacement of the main body part ( $x_1(t)$ ) and the head and neck rotational degree ( $\theta(t)$ ). The EOMs of the fore-and-aft model can be expressed by the following differential equations:

$$M\ddot{x}_1 + m_5l_n\ddot{\theta} \cos \theta - m_5l_n\dot{\theta}^2 \sin \theta + k_b(x_1 + x_0) + c_b(\dot{x}_1 + \dot{x}_0) = 0 \quad (2)$$

$$m_5l_n^2\ddot{\theta} + m_5l_n\ddot{x}_1 \cos \theta - m_5l_n g \sin \theta + k_t\theta + c_t\dot{\theta} = 0 \quad (3)$$

where  $M$  is the mass of the whole body ( $M = m_1 + m_2 + m_3 + m_4 + m_5$ ),  $l_n$  is the average distance between the shoulder and the gravity centre of the head,  $g$  is the acceleration due to gravity.

$k_t$  and  $c_t$  are the rotational spring and damper coefficients of the neck,  $k_b$  and  $c_b$  are the spring and damper coefficients between the main body and the backrest, respectively.

### 3.3 EOMs solution in the frequency domain

By taking Fourier transforms of the above EOMs the models can be analysed in the frequency domain. The Fourier transform of the vertical model EOMs (Eq. (1)) results in:

$$\{\mathbf{Z}(j\omega)\} = [-\omega^2[\mathbf{M}] + j\omega[\mathbf{C}] + [\mathbf{K}]]^{-1}\{\mathbf{F}_n(j\omega)\} \quad (4)$$

where  $\{\mathbf{Z}(j\omega)\}$  and  $\{\mathbf{F}_n(j\omega)\}$  are the complex Fourier transform vectors of  $\{\mathbf{z}\}$  and  $\{\mathbf{f}_n\}$ , respectively,  $j$  is the imaginary unit and  $\omega$  is the angular frequency. The vector  $\{\mathbf{Z}(j\omega)\}$  contains the complex displacement responses of the 5 mass segments as a function of angular frequency, and they can be represented by  $\{\mathbf{Z}_1(j\omega), \mathbf{Z}_2(j\omega), \mathbf{Z}_3(j\omega), \mathbf{Z}_4(j\omega), \mathbf{Z}_5(j\omega)\}$ .  $\{\mathbf{F}_n(j\omega)\}$  contains the complex excitation forces as a function of angular frequency as well, which is  $\{(k_1 + j\omega c_1)\mathbf{Z}_0(j\omega), 0, 0, 0, 0\}$ , where  $\mathbf{Z}_0(j\omega)$  is the complex displacement of excitation. The EOMs of the fore-and-aft model contain some nonlinear terms -  $m_5 l_n \ddot{\theta} \cos \theta$ ,  $-m_5 l_n \dot{\theta}^2 \sin \theta$ ,  $m_5 l_n \dot{x}_1 \cos \theta$ ,  $-m_5 l_n g \sin \theta$ . Small oscillations were assumed (i.e. around  $\theta = 0$ ), and the following approximation were used:  $\cos \theta = 1$ ,  $\sin \theta = \theta$ ,  $\dot{\theta}^2 \sin \theta = 0$ . The Fourier transform of the linearized equations can be expressed as follows:

$$-\omega^2 \mathbf{M} \mathbf{X}_1(j\omega) - \omega^2 m_5 l_n \boldsymbol{\theta}(j\omega) + (k_b + j\omega c_b)(\mathbf{X}_1(j\omega) - \mathbf{X}_0(j\omega)) = 0 \quad (5)$$

$$-\omega^2 m_5 l_n^2 \boldsymbol{\theta}(j\omega) - \omega^2 m_5 l_n \mathbf{X}_1(j\omega) + m_5 l_n g \boldsymbol{\theta}(j\omega) + (k_t + j\omega c_t)\boldsymbol{\theta}(j\omega) = 0 \quad (6)$$

Based on the preceding definitions, the STHT, DPMI and APM biodynamic functions for the vertical model can be derived as follows:

$$\text{STHT}_{-v} = \frac{\mathbf{Z}_5(j\omega)}{\mathbf{Z}_0(j\omega)} \quad (7)$$

$$\text{DPMI}_{-v} = \left| \frac{(k_1 + j\omega c_1)[\mathbf{Z}_0(j\omega) - \mathbf{Z}_1(j\omega)]}{j\omega \mathbf{Z}_0(j\omega)} \right| \quad (8)$$

$$\text{APM}_{-v} = \left| \frac{\text{DPMI}_{-v}}{j\omega} \right| = \left| \frac{(k_1 + j\omega c_1)[\mathbf{Z}_0(j\omega) - \mathbf{Z}_1(j\omega)]}{-\omega^2 \mathbf{Z}_0(j\omega)} \right| \quad (9)$$

Considering the Eqs. (5) and (6) of the fore-and-aft model in a similar manner, the STHT, DPMI and APM biodynamic functions for the fore-and-aft model can be derived as follows:

$$\text{STHT}_{-f} = \frac{l_n \boldsymbol{\theta}(j\omega) + \mathbf{X}_1(j\omega)}{\mathbf{X}_0(j\omega)} \quad (10)$$

$$\text{DPMI}_{-f} = \left| \frac{(k_b + j\omega c_b)(\mathbf{X}_1(j\omega) - \mathbf{X}_0(j\omega))}{j\omega \mathbf{X}_0(j\omega)} \right| \quad (11)$$

$$\text{APM}_{-f} = \left| \frac{\text{DPMI}_{-f}}{j\omega} \right| = \left| \frac{(k_b + j\omega c_b)(\mathbf{X}_1(j\omega) - \mathbf{X}_0(j\omega))}{-\omega^2 \mathbf{X}_0(j\omega)} \right| \quad (12)$$

#### 4 MODEL PARAMETER IDENTIFICATION

Model parameters were identified using curve fitting methods formulated in Matlab (version 2011b). The Least Absolute Residual (LAR) method and the 'Trust-Region' algorithm are used. The fitting process involves the solution of a multivariable optimization function comprising the root mean square errors between the computed values using the model and those target values measured experimentally (Tables 1 and 2). In the vertical model there are 17 unknown parameters in total, which can be represented in a vector as:  $p_v = [c_1, c_2, c_3, c_4, c_{41}, c_5, k_1, k_2, k_3, k_4, k_{41}, k_5, m_1, m_2, m_3, m_4, m_5]^T$ . Since the mass ( $m_1, m_2, m_3, m_4, m_5$ ) are shared parameters, in the fore-and-aft model the unknown parameters vector can be expressed as:  $p_f = [c_b, c_t, k_b, k_t, l_n]^T$ . The vectors  $p_v$  and  $p_f$  are identified separately by fitting the biodynamic functions in Eqs. (7-12). 73.6% (percentage of body mass supported by the seat for erect seating posture) of the whole body weight (75 kg) is used for the total model mass (i.e. 73.6% of 75kg =55.2kg). The identified model parameters are listed in Table 3.

Model parameters	Identified values	Model parameters	Identified values
Head and neck mass $m_5$ (kg)	5.6	Damping coefficient $c_5$ (Ns/m)	977.4
Upper torso mass $m_4$ (kg)	20.3	Damping coefficient $c_b$ (Ns/m)	621.9
Arms mass $m_3$ (kg)	8.0	Damping coefficient $c_t$ (Ns/m)	18.9
Viscera mass $m_2$ (kg)	9.2	Stiffness coefficient $k_1$ (N/m)	120123.3
Lower torso mass $m_1$ (kg)	10.0	Stiffness coefficient $k_2$ (N/m)	5300.3
Average distance $l_n$ (m)	0.19	Stiffness coefficient $k_3$ (N/m)	13177.7
Damping coefficient $c_1$ (Ns/m)	2376.4	Stiffness coefficient $k_4$ (N/m)	9151.1
Damping coefficient $c_2$ (Ns/m)	675.8	Stiffness coefficient $k_{41}$ (N/m)	128198.6
Damping coefficient $c_3$ (Ns/m)	145.8	Stiffness coefficient $k_5$ (N/m)	292010.0
Damping coefficient $c_4$ (Ns/m)	1797.7	Stiffness coefficient $k_b$ (N/m)	9925.7
Damping coefficient $c_{41}$ (Ns/m)	4023.2	Stiffness coefficient $k_t$ (N/m)	772.4

Table 3: Identified parameter values for the vertical and fore-and-aft human body models.

#### 5 SIMULATION RESULTS

After all the model parameters have been identified, the magnitude and phase responses of the STHT, DPMI and APM biodynamic functions were simulated in Matlab and the results are listed in Table 4. To evaluate the goodness-of-fit (GOF) of the presented models, the ratio of the root-mean-square error to the mean value was calculated using the following equation:

$$GOF = 1 - \frac{\sqrt{\sum (\mathbf{y}_m - \mathbf{y}_c)^2 / (N - 2)}}{\sum \mathbf{y}_m / N} \quad (13)$$

where  $\mathbf{y}_m$  and  $\mathbf{y}_c$  are the measured target data and calculated value, respectively.  $N$  is the number of the measured target data points. The  $GOF$  statistic can take on any value less than or equal to 1, with a value closer to 1 indicating a better fit ( $GOF$  less than 0 is marked by  $\sim$ ).

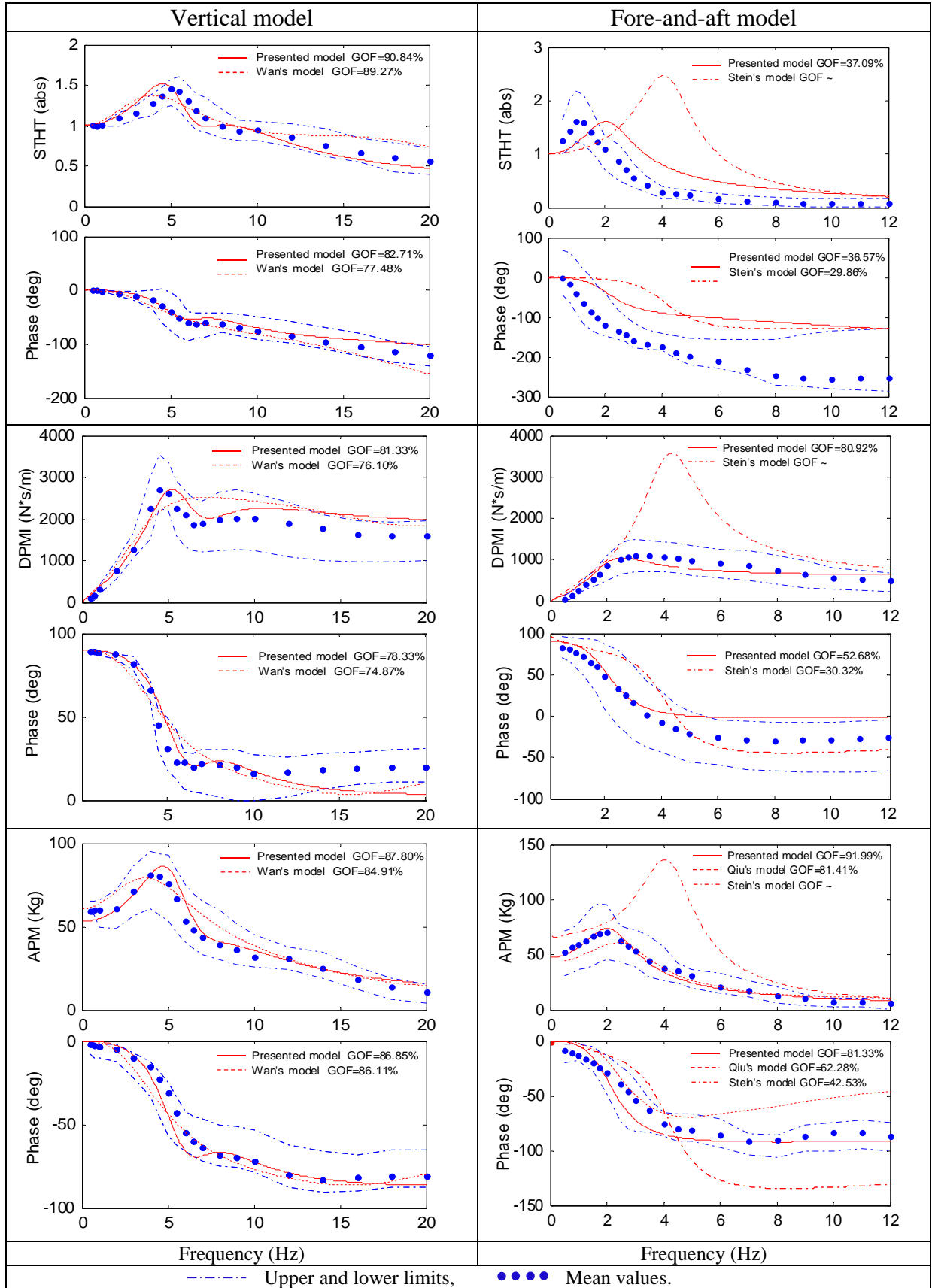


Table 4: Simulation results and comparisons of the seated human body models.

## 6 DISCUSSION

As shown in the simulation results, three previous human body models were selected for comparison: a 4-DOF linear vertical model developed by Wan and Schimmels [13], which has been found to provide the highest average of goodness-of-fit in [4] is chosen for the vertical model comparison; a 5-DOF fore-and-aft apparent mass model (for APM function comparison only) developed by Qiu and Griffin [14] and a 2-DOF fore-and-aft model developed by Stein et al. [15] are selected for the fore-and-aft model comparison. Because of the variations of the synthesized target data used in these models, the calculated GOF of the models may not be the original presented values. The measurement condition of the target data used in Stein's model varies somewhat from those of the synthesized target data in the fore-and-aft direction. However, the target data used in Wan and Qiu's models are very close to the synthesized target data in this study.

From the simulation results, the vertical seated human models show a higher average goodness-of-fit than the fore-and-aft models in both the magnitude and phase responses of the STHT, DPMI and APM functions. The presented vertical model provides 90.84% GOF and 82.71% GOF for the STHT magnitude and phase responses, 81.33% GOF and 78.33% GOF for the DPMI magnitude and phase responses, 87.80% GOF and 86.85% GOF for the APM magnitude and phase responses, respectively. This indicates that a better overall GOF is achieved for predicting the above biodynamic functions for the seated human body under vertical vibration. The results also show that peaks occur at about 5 Hz in the magnitude responses of all the three functions, which indicates the ability to predict identical primary resonant frequencies. In addition, the presented vertical model predicts a second resonant frequency around 8 Hz which is observed in the target data.

The fore-and-aft model simulation results show that a relatively large deviation is exhibited. The presented model provides the highest match for the APM function, with 91.99% GOF magnitude and 81.33% GOF phase fits. The GOF for the DPMI function is relatively lower and the prediction for the STHT function is the poorest. Because of the large differences between the measurement data, Stein's model shows poor matches for all the three functions. It is noted that the quantity of reported experimental data for the seated human body responses in the fore-and-aft direction is considerably less than the data in the vertical direction. More measurement data is needed to guide and validate the human body modelling in the fore-and-aft direction. It is also noted that the phase responses of the three biodynamic functions are usually measured in experimental studies; however, they are rarely evaluated and analysed in human body modelling studies. The phase responses of the biodynamic functions are evaluated in this study since the phase responses can be equally as important as the magnitude responses, if not more so, when it comes to human body vibration cancellation.

## 7 CONCLUSION

This study presents a lumped-parameter biodynamic model of a seated human body exposed to low frequency whole-body vibration in both the vertical and fore-and-aft directions. Model parameters are identified using curve fitting methods and the STHT, DPMI and APM biodynamic magnitude and phase response functions are simulated in Matlab. The goodness-of-fit of the presented model is evaluated graphically and statistically, and the results show that an improved fit with the synthesized experimental data is achieved. Through the model, the biodynamic behaviour of the seated human body can be observed in a more comprehensive way.

**REFERENCES**

- [1] M.H. Pope, D.G. Wilder and M.L. Magnusson, A review of studies on seated whole body vibration and low back pain. *Proceedings of the Institution of Mechanical Engineers, Part H: Journal of Engineering in Medicine*, 213-435, 1999.
- [2] G.S. Paddan, M.J. Griffin, A review of the transmission of translational seat vibration to the head. *Journal of Sound and Vibration*, 215(4), 863-882, 1998.
- [3] P.E. Boileau, S. Rakheja, Whole-body vertical biodynamic response characteristics of the seated vehicle driver measurement and model development. *International Journal of Industrial Ergonomics*, 22, 449-472, 1998.
- [4] C.-C. Liang, C.-F. Chiang, A study on biodynamic models of seated human subjects exposed to vertical vibration. *International Journal of Industrial Ergonomics*, 36, 869-890, 2006.
- [5] B. Hinz, G. Menzel, R. Blüthner and H. Seidel, Seat-to-head transfer function of seated men—determination with single and three axis excitations at different magnitudes. *Industrial Health*, 48, 565–583, 2010.
- [6] T.E. Fairley, M.J. Griffin, A test method for the prediction of seat transmissibility. *Society of Automotive Engineers International Congress and Exhibition Paper*, 860047, 1986.
- [7] B. Hinz, H. Seidel, The nonlinearity of the human body's dynamic response during sinusoidal whole body vibration. *Industrial Health*, 25, 169-181, 1987.
- [8] P. Holmlund, R. Lundström, Mechanical impedance of the human body in the horizontal direction. *Journal of Sound and Vibration*, 215(4), 801-812, 1998.
- [9] N.J. Mansfield, M.J. Griffin, Effects of posture and vibration magnitude on apparent mass and pelvis rotation during exposure to whole-body vertical vibration. *Journal of Sound and Vibration*, 253, 93-107, 2002.
- [10] M.G.R. Toward, M.J. Griffin, Apparent mass of the human body in the vertical direction: effect of a footrest and a steering wheel. *Journal of Sound and Vibration*, 329, 1586-1596, 2010.
- [11] Y. Qiu, M.J. Griffin, Biodynamic responses of the seated human body to single-axis and dual-axis vibration. *Industrial Health*, 48, 615-627, 2009.
- [12] T.E. Fairley, M.J. Griffin, The apparent mass of the seated human body: vertical vibration. *Journal of Biomechanics Engineering*, 109, 148-153, 1987.
- [13] Y. Wan, J.M. Schimmels, A simple model that captures the essential dynamics of a seated human exposed to whole body vibration. *Advances in Bioengineering, ASME, BED*, 31, 333-334, 1995.
- [14] Y. Qiu and M.J. Griffin, Modelling the fore-and-aft apparent mass of the human body and the transmissibility of seat backrests. *Vehicle System Dynamics: International Journal of Vehicle Mechanics and Mobility*, 49(5), 703-722, 2011.
- [15] G.J. Stein, P. Múčka, R. Chmúrny, B. Hinz and R. Blüthner, Measurement and modelling of x-direction apparent mass of the seated human body—cushioned seat system. *Journal of Biomechanics*, 40, 1493-1503, 2007.